ELSEVIER

Journal of Molecular Liquids 121 (2005) 80–87

journal of MOLECULAR LIQUIDS

www.elsevier.com/locate/molliq

Low temperature Raman study of stable and metastable structures of phenylacetylene in benzene. Vibrational dynamics in undercooled liquid solutions, crystals, and glassy crystals

B. Brożek-Płuska[a,*], G. Waliszewska[a], M. Jackowicz[a], S. Kuberski[b], R. Zarzycki[b], G. Janowska[c], H. Abramczyk[a]

[a]*Technical University, Institute of Applied Radiation Chemistry, Laboratory of Laser Molecular Spectroscopy, 93-590 Łódź, Wróblewskiego 15 street, Poland*

[b]*Technical University, Faculty of Process and Environmental Engineering, 90-924 Łódź, Wolczanska 175 street, Poland*

[c]*Technical University, Institute of Polymers, 90-537 Łódź, Stefanowskiego 12/16 street, Poland*

Received 19 May 2004; accepted 8 October 2004
Available online 19 February 2005

Abstract

Raman spectra of the ν_s(≡C–H) and ν_s(C≡C) stretching modes as well as Raman spectra in the lattice region 15–200 cm^{-1} of phenylacetylene (PA) dissolved in benzene in homogeneous liquid solutions, undercooled liquid state, crystal, and glassy matrices as a function of concentration, temperature, and quenching rate have been recorded in the temperature range of 77–293 K. The optical measurements were complemented by the differential scanning calorimetry (DSC) measurements. One has been demonstrated that the Raman spectroscopy combined with the DSC method is a powerful tool to obtain information about the nature of phase transitions at the molecular level. The results reveal some dramatic changes with concentration, temperature, and quenching rate and are of potential relevance both to fundamental condensed phase modelling and to liquid crystal technology. We have discussed the origin of a vibrational substructure observed for the stretching modes of phenylacetylene in benzene. We have found that the components of the vibrational structure correspond to stable, equilibrium crystal phase, and two non-equilibrium glassy crystal phases.

Low temperature polymorphism of phenylacetylene–benzene mixtures in a broad temperature range of 77–293 K has been characterized. We have found that the low temperature polymorphism of phenylacetylene strongly depends on concentration, temperature, and quenching rate. We hope this paper is an important step in understanding mechanisms of nucleation and irreversible phase transitions.

Keywords: Raman spectra; Phenylacetylene; Benzene

1. Introduction

The development of techniques that control fast cooling rate such as laser quenching, cold compression of crystals, solvent evaporation, and many others has led to the enormous progress in materials science and the discovery of new glasses. Many engineering materials of technological significance such as plastics, optical fibers, some metallic substances, and alloys can be produced as amorphous solids. Nearly all materials with every class of bonding can be frozen into a glassy solid or a crystalline state depending on the rate of cooling used in the process of solidification.

The technological routes to produce crystals, metastable liquids, or amorphous glasses have been known for millennia but we still do not know much about molecular mechanisms responsible for the glass transition, nucleation, structural relaxation of metastable liquids and interplay of kinetics and thermodynamics in generation of different phases.

* Corresponding author.
E-mail address: brozek@mitr.p.lodz.pl (B. Brożek-Płuska).

0167-7322/$ - see front matter © 2004 Elsevier B.V. All rights reserved.
doi:10.1016/j.molliq.2004.10.036

Although a great deal of effort has been expanded to explain the molecular properties of undercooled liquids, amorphous glasses, and crystal-forming liquids [1–6], there is no theory that accurately describes the behaviour of any system over the full temperature range in which the relaxation times cover 15 orders of magnitude [7–9]. Moreover, most experimental methods can cover only a narrow window on the time scale and the same indicator of molecular properties cannot be used over a broad temperature range for different thermodynamics states for most of the experimental methods. In contrast, Raman spectroscopy is a method that allows to monitor various thermodynamic states over a very broad temperature range.

Recently, we have studied structural and dynamical aspects of equilibrium and non-equilibrium phase transitions for phenylacetylene in various solvents monitoring them by the low temperature Raman spectroscopy [10,11].

We will show that vibrational static properties and vibrational dynamics recorded by Raman spectroscopy are powerful indicators of phase transitions and molecular structure generated during cooling of a sample. In contrast to liquids and crystals, there is a limited number of experimental data on vibrational dynamics in thermodynamic states that are out of equilibrium such as supercooled liquids and glasses or glassy crystals [1–5,10–14]. The dynamics including vibrational dynamics of undercooled liquids are of particular interest since interactions are stronger than in the normal liquid state.

In this paper we hope to understand the competition between the various stable and metastable phases in phenylacetylene solutions generated during the phase transitions that depend on factors such as concentration, temperature, interactions with impurities as well as a quenching rate. Phenylacetylene derivatives are of particular interest with regard to the most recent liquid crystal technologies including PDLC (polymer dispersed liquid crystals) and other confined geometries formed by polymers or porous network [15]. Phenylacetylene seems to be a suitable simple model for the exploration of different stable and metastable phases. To understand the structure and dynamics of phenylacetylene solution in liquid and solid phases at a molecular level we have used vibrational Raman spectra as a physical probe to study them. We have recorded the Raman spectra of the ν_s(≡C–H) and ν_s(C≡C) stretching modes as well as Raman spectra in the lattice region 15–200 cm^{-1} of phenylacetylene in benzene in the temperature range of 77–293 K as a function of concentration, temperature, and a quenching rate. Recently we have characterized the polymorphism and identified the phases of phenylacetylene generated in acetonitrile and methylcyclohexane [10,11].

The aim of the present study is to characterize the polymorphism and to identify the phases that are generated in PA–benzene mixtures and compare them with those generated in PA–acetonitrile and PA–methylcyclohexane systems.

2. Experiment

Spectrograde benzene and phenylacetylene were purchased from Aldrich. Benzene was used without further purification. Phenylacetylene was distillated under vacuum before preparing solutions.

The Raman spectra were recorded in the cryostat (Oxford Instruments) and commercial glass ampoules were mounted in a special cell arrangement.

Raman spectra were measured with Ramanor U1000 (Jobin Yvon) and Spectra Physics 2017-04S argon ion laser operating at 514 nm. The Raman spectra corresponding to the lattice region 15–200 cm^{-1} and to the C≡H stretching mode as well as the VV Raman spectra of the C≡C stretching mode of PA in benzene were recorded in a broad temperature range from 293 to 77 K.

The DSC traces were measured during heating of the frozen samples as well as cooling of the liquid solution at a rate of 0.5 K/min at 1 atm pressure with Netzsch DSC 200 instrument in ampoules of 80 mg.

More experimental details are given in our recent paper on this subject [11].

3. Results

Fig. 1a–c show the DSC scans of neat PA, neat benzene, and PA in benzene solution, respectively. Fig. 1a shows a large melting-like endotherm signal at around T^{m}_{PA}=240 K corresponding to the solid phase–liquid transition of PA and a large exotherm signal at T_{PA}=203 K corresponding to the undercooled liquid–solid phase transition of PA. The undercooled liquid represents a liquid state below the melting point temperature. Fig. 1b shows a melting-like endotherm signal with maximum at around T^{m}_{B}=283 K corresponding to the solid phase–liquid transition of benzene and a large exotherm signal at T_{B}=258 K corresponding to the undercooled liquid–solid phase transition of benzene. In contrast to Fig. 1a–b one can see from Fig. 1c that there are three peaks for the PA–benzene mixture on the endotherm curve, at 225 K, 239 K, and 251 K. The peak at 251 K corresponds to the solid–liquid benzene melting phase transition. The two melting-endotherm signals for PA at 225 K and 239 K correspond to PA solid–PA liquid phase transitions and demonstrate that there are two distinct phases generated during cooling of the PA–benzene system [PA(I) and PA(II)]. The pattern of behaviour presented in Fig. 1c on the exotherm curve illustrates that the PA–benzene homogenous liquid mixture becomes a heterogeneous system at lower temperatures that solidifies into separate phases corresponding to PA and benzene, respectively. The solidification of benzene in PA–benzene mixture occurs at around T_{B}=229 K, whereas PA still exists as a undercooled liquid down to T_{PA}=201 K. Fig. 1c presents the DSC scans for PA concentration c=3.2 mol/dm^{3} but a similar pattern of behaviour has been

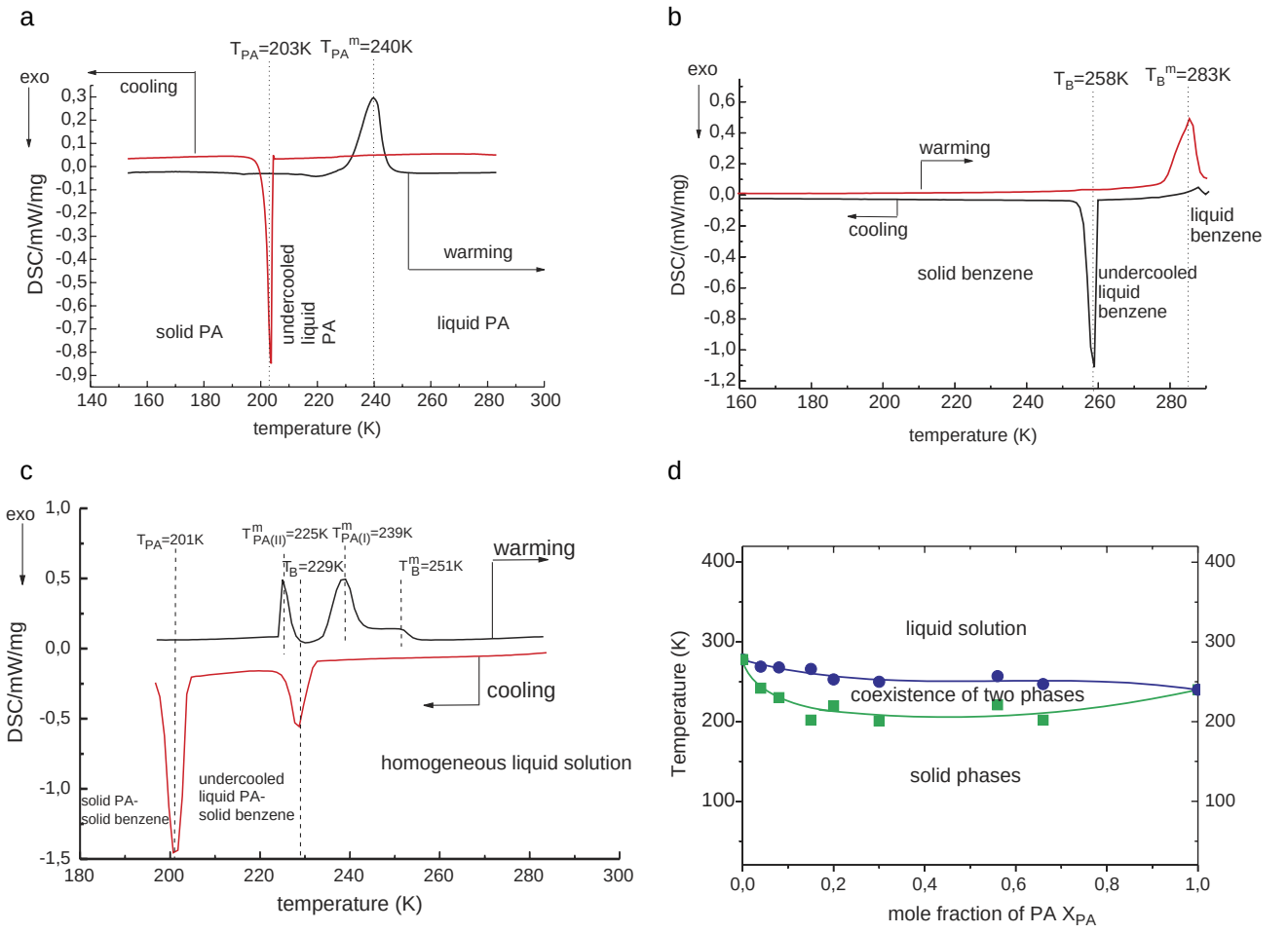

Fig. 1. Differential scanning calorimetry (DSC) signals for cooling and warming of the sample (a) neat phenylacetylene, (b) neat benzene, (c) phenylacetylene in benzene (c=3.2 mol/dm^3, mole fraction of PA, x_{PA}=0.3), (d) phase diagram for PA–benzene system as a function of PA mole fraction x_{PA}.

recorded for PA–benzene solutions in a broad concentration range. The $T^{m}_{PA(II)}$ and the T^{m}_{B} melting-like endotherm temperatures have been used to create the phase diagram for PA–benzene system as a function of the mole fraction of PA at the constant atmospheric pressure as is shown in Fig. 1d.

Fig. 2 shows the Raman band shapes of the stretching mode ν_s(≡C–H) of PA in benzene as a function of temperature. One can see from Fig. 2 that the two phases of PA monitored by the DSC warning signals and corresponding to the temperatures at 225 K and 239 K on the exotherm Fig. 1c can be easily identified in the Raman spectra features. Indeed, the broad, structureless band above 200 K corresponding to liquid PA transforms into a narrow peak at around 3264 cm^{-1} [PA(I)] and a weak, broad band at around 3276 cm^{-1} at 201 K [PA(II)]. Moreover, the temperature of 201 K at which the spectral changes occur is identical to that obtained from the DSC cooling measurements in Fig. 1c. To identify the PA solid phases corresponding to the bands at 3264 cm^{-1} and 3276 cm^{-1} we have compared in Fig. 3 the Raman spectrum for PA in benzene with those obtained in our previous papers for PA in methylcyclohexane [10] and acetonitrile [11]. One can see that the peak at 3264 cm^{-1} for PA in benzene is observed at the similar position (3261 cm^{-1}) for PA in acetonitrile [11] whereas the broad band may correspond to

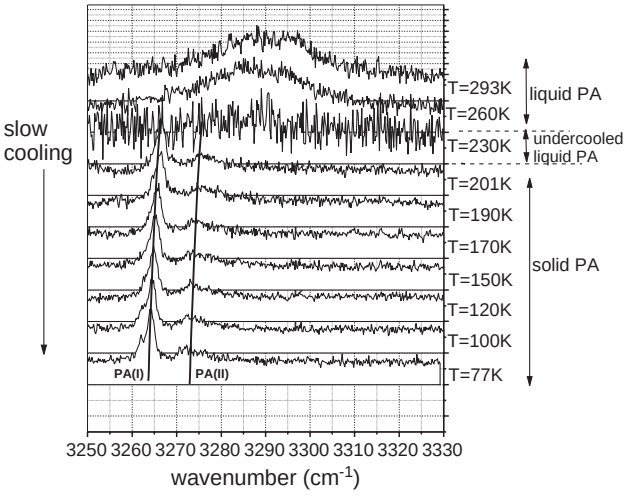

Fig. 2. Raman spectra of the ν_s(≡C–H) mode of phenylacetylene in benzene (c=3.2 mol/dm^3, mole fraction of PA, x_{PA}=0.3) as a function of temperature (slow cooling, 0.5 K/min).

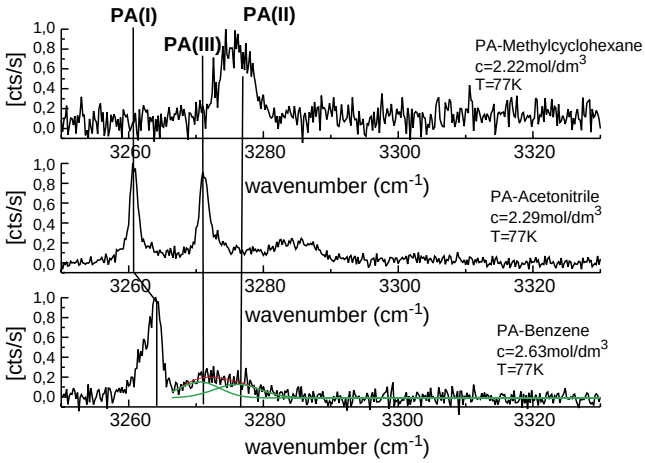

Fig. 3. Raman spectra of the ν_s(≡C–H) mode of phenylacetylene in benzene, in acetonitrile, in methylcyclohexane at 77 K (slow cooling).

that in PA–methylcyclohexane system at 3276 cm^{-1} [10]. We have proved [11] that the peak at around 3261 cm^{-1} has evidently crystalline origin as it exhibits the Davydov splitting that represents the interactions between the PA molecules in the crystal unit cell. Therefore we have assigned the peak at 3264 cm^{-1} to the crystalline equilibrium phase of PA in benzene. The broad band at 3276 cm^{-1} observed in PA–methylcyclohexane solutions has been identified as a glassy crystal phase (Fig. 3) [10]. Glassy crystals have translational order and reorientational disorder, but the reorientational energy distribution deviates from the equilibrium for a given temperature in contrast to plastic crystals. Therefore, we have assigned the broad band (3276 cm^{-1} at 201 K in Fig. 2) for PA in benzene to a non-equilibrium glassy crystal phase similar to that generated in methylcyclohexane. The comparison between the different patterns of solidification of PA in various solvents provides interesting findings about mechanisms of nucleation. Fig. 4 shows the DSC signals obtained during warming for PA–benzene, PA–acetonitrile and PA–methylcyclohexane mixtures. The comparison between these solvents leads to a clear conclusion that PA–benzene and PA–methylcyclohexane systems form heterogeneous mixtures at low temperatures. However, there is a significant difference in the solidification conditions due to the different melting temperatures of the solvents. Benzene begins to crystallize whereas PA still exists as a liquid in contrast to PA in methylcyclohexane (MCH) where the situation is reversed. In contrast to PA in benzene and methylcyclohexane both PA and acetonitrile have nearly identical melting temperatures. Comparing the intensities of the Raman components at 3264 cm^{-1} and around 3276 cm^{-1} in Figs. 2 and 3 with the integral intensities of the DSC signals in Fig. 4 we can state that both crystallization and amorphization occur in PA in benzene mixture in contrast to PA–methylcyclohexane mixture where the amorphous glassy crystal phase is the only generated phase.

The crystallization of PA in benzene seems to dominate because the benzene crystals at higher temperatures may act as centres of nucleation for liquid PA. Contrary, PA molecules in MCH solution have no centres of nucleation because MCH exists as a liquid down to T^{m}_{MCH}=145 K. This is a reason why PA molecules in MCH choose amorphous route of solidification rather than crystallization.

Having reached this point when we suspect which phases are preferentially generated in PA–benzene mixture, we

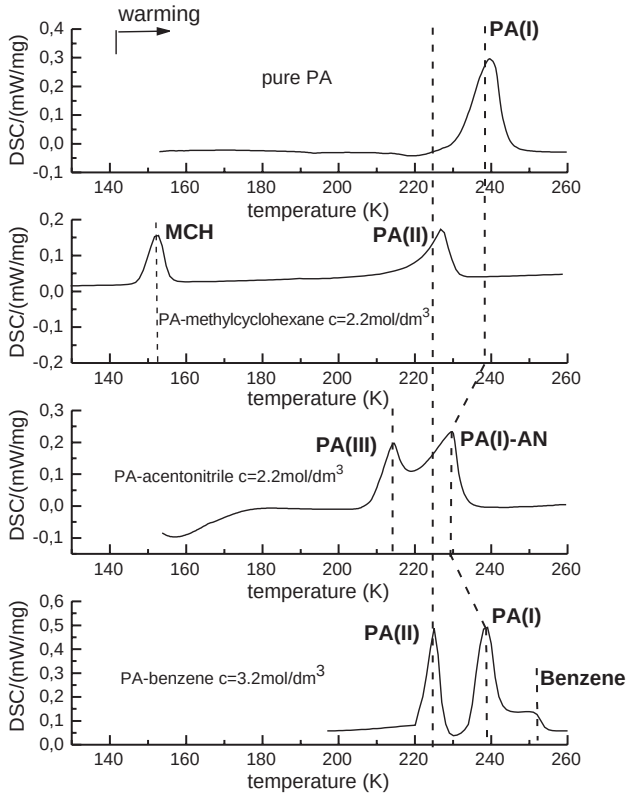

Fig. 4. Differential scanning calorimetry (DSC) signals of the sample (a) neat phenylacetylene, (b) phenylacetylene in methylcyclohexane c=2.2 mol/dm^3, (c) phenylacetylene in benzene (c=3.2 mol/dm^3), (d) phenylacetylene in acetonitrile c=2.2 mol/dm^3. AN—acetonitrile, MCH—methylcyclohexane, PA—phenylacetylene.

have explored the influence of quenching rate on polymorphism of the samples generated in PA–benzene mixtures. We have found that in contrast to PA–methylcyclohexane and PA–acetonitrile mixtures [10,11] the nature and the number of generated phases for the PA–benzene system depend strongly on the quenching rate.

Lets us recall that for the slow cooling (0.5 K/min) the solidification is dominated by the crystallization of PA [PA(I)] with some contribution from an amorphous glassy crystal phase [PA(II); Fig. 2]. Fig. 5a shows the Raman bands at 77 K of the stretching mode ν_s(≡C–H) of PA in benzene at 77 K for the rapid quenching. The first observation that one makes confronting the results from Figs. 5a and 2 is that the amorphous phase may dominate over the crystal for the rapid cooling in contrast to the crystal phase that is always favoured for the slow cooling. For the rapid cooling the crystal phase of PA [PA(I)] is represented by a single narrow peak at around 3264 cm^{-1} like for the slow cooling whereas the broad bands at 3270 cm^{-1} and 3279 cm^{-1} with the bandwidths of 7.9 cm^{-1} and 8.4 cm^{-1} must obviously correspond to disordered amorphous phases (Fig. 5a and b) They are significantly broader than the crystalline component at 3264 cm^{-1} for the same ν_s(≡C–H) oscillator, which has the bandwidth of 3.37 cm^{-1}. Therefore, in contrast to the slow cooling when only one crystal phase PA(I) and glassy phase [PA(II)] are generated (Fig. 2), the fast cooling leads to generation of three distinct phases: the crystal phase PA(I) and two glassy phases [PA(II) and PA(III)]. These three phases are clearly evident from the results in Fig. 7 that will be discussed later, where the S/N ratio is much higher.

However, it is of concern that reproductibility in Fig. 5a illustrates an apparent lack of correlation between the PA concentration and the number of phases. Indeed, for the similar concentrations of 2.33, 2.91, 2.94 mol/dm^3 we observe the different patterns of behaviour. For c=2.33 mol/dm^3 the PA structure in benzene is dominated by the crystal phase at 3264 cm^{-1} [PA(I)], for c=2.91 mol/dm^3 the mixture of the crystal phase PA(I) and of the two disordered phases at 3270 cm^{-1} and 3279 cm^{-1} [PA(III) and PA(II)] is generated whereas the PA structure for c=2.94 mol/dm^3 represents entirely disordered phase PA(II). The results from

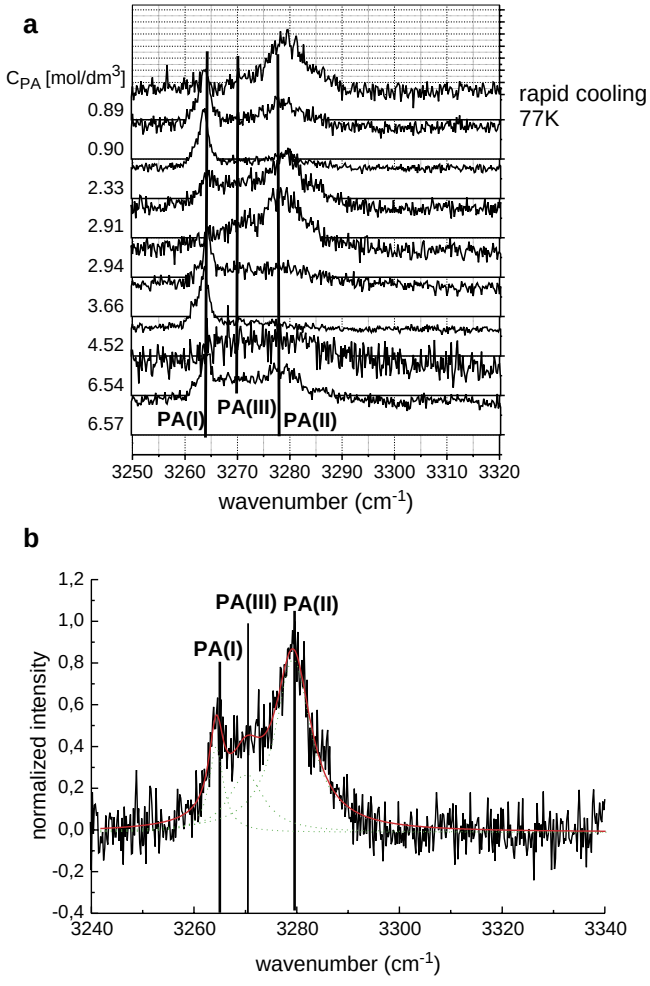

Fig. 5. (a) Raman spectra of the ν_s(≡C–H) mode of phenylacetylene in benzene as a function of concentration (rapid cooling, immersing in liquid nitrogen), (b) fitting of the band profile for c=2.91 mol/dm^3 at 77 K (rapid cooling, immersing in liquid nitrogen).

Fig. 5a simply illustrate that in contrast to the slow cooling procedure the rapid quenching is governed by some additional effects such as concentration and/or temperature gradients that cannot be fully controlled during immersing of the samples in liquid nitrogen. Despite of this drawback we have decided to present the results in Fig. 5a because they provide an excellent illustration about competition between the different phases.

To get a deeper insight into the PA structures at the molecular level represented by the bands at 3264, 3270, and 3279 cm^{-1} which correspond to the three phases: PA(I), PA(II), and PA(III) we have recorded the low-frequency Raman spectra of PA–benzene mixtures in the 15–200 cm^{-1} region. It is well-known that this region is very sensitive to molecular motions occurring in the systems characterized by high degree of translational order and may help to identify the crystal phases. Lack of the lattice bands in this region indicates that the glassy phase has been generated. In contrast, sharp and narrow lattice peaks in the low-frequency spectrum signalise that a translationally and reorientationally ordered crystal phase has been generated. Broad, structureless bands represent an intermediate case with translational order typical for crystals and reorientational disorder typical for glasses or plastic crystals.

Fig. 6 shows the low-frequency Raman spectra for PA in benzene as a function of concentration at 77 K for the same samples, and the identical experimental conditions of temperature and quenching as in Fig. 5a. What kind of insight can one gain from comparing Fig. 6 with Fig. 5a? The first observation that one makes when confronting the results is an excellent correlation between the spectra in these two regions. Indeed, a broad, structureless band with no evidence of the lattice crystal peaks in Fig. 6 for c=6.54 mol/dm^3 that evidently represents an amorphous translationally disordered phase corresponds to the broad band in Fig. 5a with no contribution from the crystal peak at 3264 cm^{-1}. In contrast one can see the sharp phonon peaks in Fig. 6 indicating evidently lattice crystalline structure for

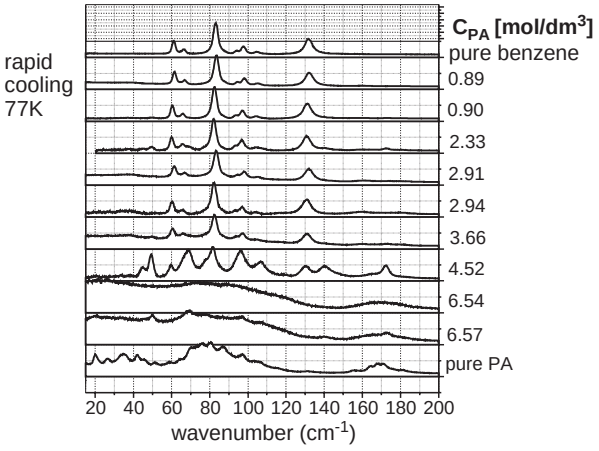

Fig. 6. Raman spectra of the lattice region 15–200 cm^{-1} for phenylacetylene in benzene as a function of concentration at 77 K (rapid cooling, immersing in liquid nitrogen).

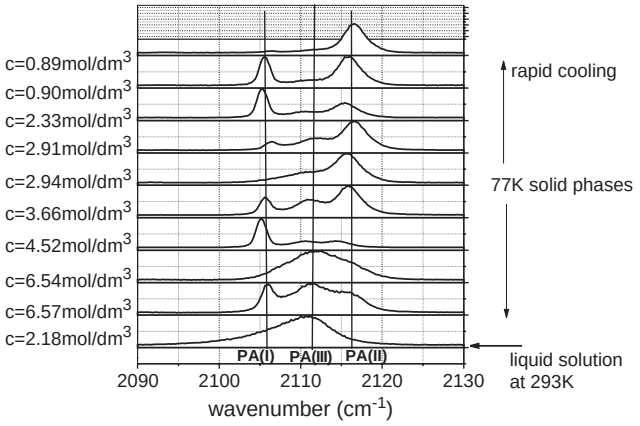

Fig. 7. Raman spectra of v_s(C≡C) stretching mode of phenylacetylene in benzene as a function of concentration at 77 K (rapid cooling, immersing in liquid nitrogen).

PA concentration c=4.52 mol/dm^3 for which the sharp crystalline peak at 3264 cm^{-1} is also observed in Fig. 5a. The crystalline phase of PA generated for c=0.90 and 2.33 or 3.66 mol/dm^3 (see Fig. 5a) is demonstrated by the weak peaks centred at 50 cm^{-1}, 70 cm^{-1}, and 173 cm^{-1} in Fig. 6. However, for concentrations lower than c=4.52 mol/dm^3 the properties of PA are not clearly seen in this spectral region because the low-frequency Raman spectra in Fig. 6 are dominated by the spectral features of benzene due to higher scattering cross-section.

To ascertain that the spectacular features observed for the v_s(≡C–H) oscillator illustrate the different phases of PA we have recorded the Raman spectra for another oscillator. The Raman spectra for the stretching mode v_s(C≡C) of PA in benzene were recorded as a function of concentration at 77 K for the same samples and identical experimental conditions as in Figs. 5a and 6. The results are shown in Fig. 7. Again, the pattern of behaviour that emerges from Fig. 7 proves an excellent correlation with the results in Figs. 5a and 6. For example, a broad, structureless band of the v_s(C≡C) oscillator at 2110 cm^{-1} is observed for the same concentration (c=6.54 mol/dm^3) as for the v_s(≡C–H) oscillator in Fig. 5a and for the low-frequency region in Fig. 6 with no evidence of crystal ordering. Contrary, the crystal phase of PA for c=4.52 mol/dm^3 is represented by a single peak at 3264 cm^{-1} in Fig. 5a as well as a single peak at 2105 cm^{-1} for the v_s(C≡C) oscillator in Fig. 7. Therefore, the red shifted band at 2105 cm^{-1} corresponds to that of 3264 cm^{-1} and they both represent the crystal phase of PA [PA(I)]. The most blue shifted component centred at 2116 cm^{-1} corresponds to that at around 3279 cm^{-1} (rapid cooling) and 3276 cm^{-1} (slow cooling) and they represent the amorphous glassy crystal phases of PA [PA(II)]. The third component at 2110 cm^{-1} in Fig. 7 corresponds to that at 3270 cm^{-1} in Fig. 5a and b. The peak at 3270 cm^{-1} observed for the rapid cooling in Fig. 5a and b has not been recorded for the slow cooling, Fig. 2. The nature of PA(III) phase remains still unknown.

4. Discussion

Raman spectroscopy measures the fluctuations in the vibration-modulated polarizabilities. If we denote by A a Cartesian component of the collective polarizability tensor in the sample, then the spectral Raman band for the vibrational mode v is related to the time correlation function (TCF; [16,17])

$$C_v(t) = \sum_{i=1}^{N}\sum_{j=1}^{N} \langle A'_{iv}(0)Q_{iv}(0)A'_{jv}(t)Q_{jv}(t)\rangle, \quad (1)$$

where Q_{iv} is the vibrational coordinate for this mode in the ith molecule and $A'_{iv}=[\partial A/\partial Q_{iv}]_{Q_{iv}}=0$.

The vibrational TCF $C_{\mathrm{vib}}(t)$ in condensed phases decays through vibrational dephasing and vibrational energy (population) relaxation. Dephasing occurs through fluctuations in vibrational frequencies due to differences in vibrational frequencies of molecules in different molecular environments. The decay time T_2 obtained from the homogeneous vibrational line shape is related to the pure dephasing time T_2^* and population relaxation time T_1 by

$$\frac{1}{T_2} = \frac{1}{T_2^*} + \frac{1}{2T_1} \quad (2)$$

The part of dephasing due to fast fluctuations in vibrational frequencies gives rise to homogeneous broadening in the vibrational line shape. The portion of dephasing occurring due to static or slowly relaxing disorder gives rise to inhomogeneous broadening in the experimental vibrational line shape. Therefore, the band widths are related to the vibrational dephasing times and provide valuable information about vibrational dynamics.

Fig. 8 shows the Raman band width (FWHH) of the ν_s(≡C–H) mode of PA in benzene as a function of temperature for the slow cooling and concentration of c=3.2 mol/dm^3. The characteristic temperatures, T_{PA} and $T_{\mathrm{PA}}^{\mathrm{m}}$ representing the undercooled liquid PA–solid PA transition and the melting temperature for PA in PA–benzene mixture are shown on the plot. One can see that the Raman bandwidth increases monotonically with temperature decreasing down to T_{PA}=201 K. At T_{PA} the bandwidth decreases dramatically in discontinuous way followed by monotonic decrease with further temperature decreasing for the crystal phase [PA(I)] and no temperature dependence for the glassy crystal phase PA(II). The magnitudes of the bandwidths extrapolated to T=0 are 0.86 cm^{-1} [crystal PA(I)], and 5.34 cm^{-1} [glassy crystal-PA(II)] indicating evidently once again that the component at 3276 cm^{-1} represents the amorphous disordered glassy phase with respect to the 3264 cm^{-1} component that represents the crystal state. The band broadening of the band at 3276 cm^{-1} cannot come from the plasticity of the crystal since the bandwidth shows no temperature dependence. Generally, homogenous and inhomogeneous band broadening cannot be separated by the conventional Raman spectroscopy as well as by the third order nolinear Raman techniques (CARS). The separation is feasible only with nolinear echo-techniques [14,18]. However, in many cases the temperature or concentration dependences analysis makes it possible separating different band broadening mechanisms.

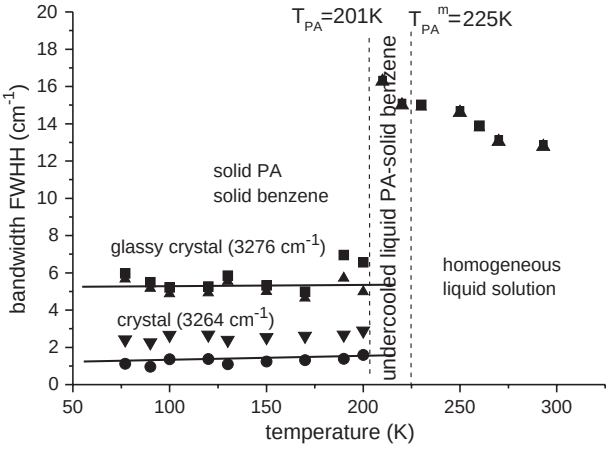

Fig. 8. Raman band width (FWHH) of the ν_s(≡C–H) stretching mode of PA in benzene as a function of temperature (c=3.2 mol/dm^3, mole fraction of PA, x_{PA}=0.3; slow cooling, 0.5 K/min), ■—experimental data for the components at 3276 cm^{-1}, ▲—data after deconvolution for the components at 3276 cm^{-1}, ●—experimental data for the components at 3264 cm^{-1}, ▼—data after deconvolution for the components at 3264 cm^{-1}.

There is no theory of vibrational dynamics that would accurately describe the behaviour of any liquid over the full temperature range in which the relaxation times cover 15 orders of magnitude because different mechanisms give different contribution in various temperature range and each of them can lead to very different temperature dependences. However, pure vibrational dephasing T_2 dominates the homogeneous line width at high temperatures. We have shown [12] that the band broadening in PA–benzene solution at 293 K is dominated by the repulsive collisions. The hard-sphere collision model [12] predicts a temperature dependence of $\Delta_{1/2} \propto \rho T^{3/2} g(\sigma)$, where ρ and $g(\sigma)$ are the density of the solution and the radial distribution function, respectively. According to the model the band width should decrease in the range 298–201 K, not increase as observed in Fig. 8. The deviation from the hard collision model indicates that additional mechanisms of band broadening begin to dominate with the decreasing temperature. Below the melting temperature for PA $T_{\mathrm{PA}}^{\mathrm{m}}$=225 K where PA exists as the undercooled liquid, the system begins to prepare for solidification and the additional dynamics features due hydrodynamics fluctuations, viscoelastic effects, and density fluctuations begin to dominate. These density fluctuations that can be determined experimentally from the structure factors S(k) via neutron or X-ray scattering are clearly visible in the Raman spectra (Fig. 2) demonstrated by the significant decrease of the signal to noise ratio for undercooled PA. The density fluctuations must lead to additional band broadening observed experimentally that

becomes more and more inhomogeneous with decreasing temperature and its magnitude reaches the maximum at T_{PA}=201 K. Much of this analysis is at present largely qualitative and reflects the fact that there is no precise theory of vibrational dynamics for this region. However, the inhomogeneous band broadening in the region of the undercooled liquid PA is probably better described by the idea of barrier-dominated behaviour on the potential energy hypersurface known as the "energy landscape" approach [7,8] than the free-volume approach with its extreme case of hard-repulsive collision picture that we have applied for the liquid solution at 293 K [12].

The dramatic decrease of the band width at T_{PA}=201 K in a discontinuous way clearly indicates that the band broadening mechanisms operating for the undercooled PA become suddenly ineffective. Indeed, after solidification into the crystal (3264 cm^{-1}) or the glassy crystal (3276 cm^{-1}) the structure gains some translational order that leads to disappearance (or a significant reduction) of inhomogeneous band broadening. Picosecond CARS low temperature studies for most crystals show nearly perfect exponential decays [19] indicating that vibrational dynamics in the crystal phase is dominated by homogenous band broadening. It was shown [14,19] that the energy relaxation T_1 is the dominant contribution to the homogenous line width at very low temperatures, where dephasing processes caused by thermal fluctuations disappear. It was found [14] that above 50 K pure dephasing T_2^* makes the major contribution to the vibrational line width. Therefore, we believe that the temperature dependence presented in Fig. 8 in the temperature range 77–200 K for the crystal (3264 cm^{-1}) component is dominated by the T_2^* processes.

5. Conclusions

A parallel use of DSC and Raman spectroscopy has allowed to reveal and characterize the low temperature polymorphism of the mixtures of phenylacetylene in benzene in the temperature range of 293–77 K. We have found that the low temperature polymorphism of phenylacetylene in benzene strongly depends on temperature and quenching rate in contrast to PA in methylcyclohexane and PA in acetonitrile.

The essential findings are as follow. The structure of PA in benzene generated at the slow cooling is dominated by the stable crystal phase PA (I) accompanied by some contribution from the glassy crystal phase [PA(II)]. In contrast, rapid temperature quenching leads to generation of the stable crystal phase [PA(I)] accompanied by the two topologically distinct glassy phases [PA(II) and PA(III)]. The stable, equilibrium crystal phase of PA is represented by the band of the ν_S(≡C–H) stretching mode centred at 3264 cm^{-1} and shows a significant plasticity at higher temperatures. The glassy phase [PA(III)] generated during the rapid cooling is represented by the components at 3270 cm^{-1} for the ν_s(≡C–H) stretching mode and at 2110 cm^{-1} for the ν_S(C≡C) stretching mode. The peaks at 3276 cm^{-1} (slow cooling)/3279 cm^{-1} (rapid cooling) for the ν_s(≡C–H) stretching mode and at 2116 cm^{-1} for the ν_S(C≡C) stretching mode have been assigned to the glassy crystal phase of PA [PA(II)].

Mechanisms of vibrational dynamics have been discussed. The temperature dependence allows to identify the dominant mechanisms of band broadening. In the range between 293 and 250 K pure dephasing T_2^* gives the major contribution to the vibrational band width with the hard collisions as a main mechanism of the homogeneous broadening. In the range 225–201 K where PA exists as the undercooled liquid the contribution from inhomogeneous band broadening increases and comes probably from the density fluctuation mechanism [20,21]. After solidification below 201 K down to 77 K the inhomogeneous broadening disappears (or is significantly reduced) and pure dephasing T_2^* makes again the major contribution to the vibrational band width.

References

[1] H. Abramczyk, K. Paradowska-Moszkowska, Chem. Phys. 262 (2001) 177.
[2] H. Abramczyk, K. Paradowska-Moszkowska, J. Chem. Phys. 24 (2001) 11221.
[3] H. Abramczyk, K. Paradowska-Moszkowska, G. Wiosna, J. Chem. Phys. 118 (2003) 4169.
[4] C. Glorieux, K.A. Nelson, G. Hinze, M/D. Fayer, J. Chem. Phys. 116 (2002) 3384.
[5] G. Hinze, D.D. Brace, S.D. Gottke, M.D. Fayer, J. Chem. Phys. 113 (2000) 3723.
[6] S.M. Silence, A.R. Duggal, L. Dhar, K.A. Nelson, J. Chem. Phys. 96 (1992) 5448.
[7] P.G. Debenedetti, F.H. Stillinger, Nature 410 (2001) 259.
[8] P.G. Debenedetti, R.J. Errington, Nature 409 (2001) 318.
[9] C.A. Angel, K.L. Ngai, G.B. McKenna, P.F. McMillan, S.W. Marton, J. Appl. Phys. 88 (2000) 3113.
[10] B. Brożek, H. Abramczyk, S. Kuberski, Chem. Phys. 280 (2002) 153.
[11] H. Abramczyk, B. Brożek, G. Waliszewska, J.P. Suwalski, J. Phys. Chem. 106 (2002) 1486.
[12] H. Abramczyk, G. Waliszewska, M. Kołodziejski, J. Phys. Chem., A 102 (1998) 7765;
H. Abramczyk, G. Waliszewska, B. Brożek, J. Phys. Chem., A 103 (1999) 7580.
[13] B. Brożek, H. Abramczyk, Chem. Phys. 250 (1999) 35.
[14] A. Tokmakoff, M.D. Fayer, Acc. Chem. Res. 28 (1995) 437B.
[15] G.P. Crawford, S. Zumer, Liquid Crystals in Complex Geometries, Tylor and Francis, London, 1996.
[16] P.A. Madden, in: D. Steele, J. Yarwood (Eds.), Spectroscopy and Relaxation of Molecular Liquids, Elsevier, Amsterdam, 1991.
[17] D.W. Oxtoby, Adv. Chem. Phys. 40 (1979) 1;
D.W. Oxtoby, Adv. Chem. Phys. 41 (1981) 487.
[18] S. Mukamel, Principles of Nonlinear Optical Spectroscopy, Oxford Universsity Press, New York, 1995.
[19] D.D. Dlott, Laer spectroscopy of solids II, in: W.M. Yen (Ed.), Topics in Applied Physics, vol. 65, Springer-Verlag, 1989, p. 167.
[20] E.W. Knapp, S.F. Fischer, J. Chem. Phys. 76 (1982) 4730.
[21] L.J. Muller, D. Vanden Bout, M. Berg, J. Chem. Phys. 99 (1993) 810.